

Combinatorics and the Rigidity of CAD Systems*

Audrey Lee-St.John

Department of Computer Science
Mount Holyoke College
South Hadley, MA 01075
astjohn@mtholyoke.edu

Jessica Sidman

Department of Mathematics and Statistics
Mount Holyoke College
South Hadley, MA 01075
jsidman@mtholyoke.edu

October 19, 2012

Abstract

We study the rigidity of *body-and-cad frameworks* which capture the majority of the geometric constraints used in 3D mechanical engineering CAD software. We present a combinatorial characterization of the generic minimal rigidity of a subset of body-and-cad frameworks in which we treat 20 of the 21 body-and-cad constraints, omitting only point-point coincidences. While the handful of classical combinatorial characterizations of rigidity focus on distance constraints between points, this is the first result simultaneously addressing coincidence, angular, and distance constraints. Our result is stated in terms of the partitioning of a graph into edge-disjoint spanning trees. This combinatorial approach provides the theoretical basis for the development of deterministic algorithms (that will not depend on numerical methods) for analyzing the rigidity of body-and-cad frameworks.

1 Introduction

We study *body-and-cad* frameworks composed of rigid bodies with pairwise coincidence, angular and distance constraints placed between geometric elements (points, lines, planes) rigidly affixed to each body. A framework is *flexible* if the bodies can move relative to each other while respecting the constraints; otherwise, it is *rigid* (see Figures 1a and 1b). A fundamental problem for both the user and the CAD software is to determine whether a system is flexible or rigid.

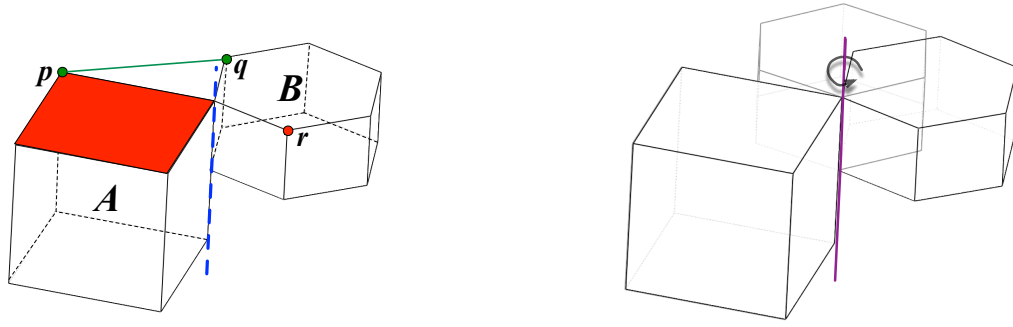
Contributions. In this paper, we present a combinatorial characterization of the generic minimal rigidity of a subset of body-and-cad frameworks: we treat 20 of the 21 constraints, omitting point-point coincidences. The equations governing point-point coincidences exhibit special algebraic behavior (see Appendix B).

Body-and-cad frameworks on n bodies without point-point coincidences can be modeled by a graph called a (k, g) -frame. Our main theorem states that generic minimal rigidity of a (k, g) -frame is equivalent to a partitioning of the graph's edge set such that each partition consists of the edge-disjoint union of 3 spanning trees. Combinatorial characterizations of rigidity typically lead to quadratic time algorithms, and we expect this result to have similar implications for the development of efficient algorithms.

Significance. Among the many classes of structures whose rigidity is studied, there are only a handful of cases for which combinatorial characterizations have been proven, with Laman's 2D bar-and-joint [10] and Tay's body-and-bar [20] results the most well-known. Furthermore, classical work has focused mainly on distance constraints. To the best of our knowledge, *ours is the first combinatorial rigidity characterization that simultaneously treats angular and other constraints.*

Motivation. In the 3D “assembly” environment of the popular CAD software SolidWorks [3], users place “mates” among parts (rigid bodies). The mates specify constraints (e.g., distance, angular, coincidences)

*Final version to appear in Symposium on Solid and Physical Modeling '12 and associated special issue of Computer Aided Design.



(a) A **minimally rigid** body-and-cad framework with (i) a line-line coincidence along the dotted blue axis, (ii) a point-plane coincidence between the red point r and shaded plane, and (iii) a point-point distance between the green points p and q .

(b) Removing the point-point distance constraint (iii) results in a **flexible** framework with 1 degree of freedom (rotation about the shared axis).

Figure 1: A 3D body-and-cad framework.

among *geometric elements* (e.g., points, lines, planes) identified on the parts. Informative feedback is important as explicit visualization of mates is difficult, and mechanical engineers are usually not experts in reasoning about the underlying geometric constraint systems.

One of the most difficult situations arises when a new mate is specified that causes an inconsistency in the design. As depicted in Figure 2, SolidWorks gives feedback in the form of an alert window and highlights a list of previous mates “overdefining” the system. This list is intended to assist the user in resolving the inconsistency, but is often too large (sometimes, the entire set of mates) to be helpful. Current software *cannot reliably detect a minimally dependent set of constraints*. Indeed, the system in Figure 2 reveals the severity of software limitations, as the lift is essentially 2-dimensional. It is composed of two “scissor” parts attached by struts connecting pairs of matching joints. Since the “scissor” parts must move identically, analysis can be reduced to considering a single “scissor,” which itself is a planar mechanism. The development of a complete **rigidity theory** would provide a rigorous mathematical understanding of these geometric systems.

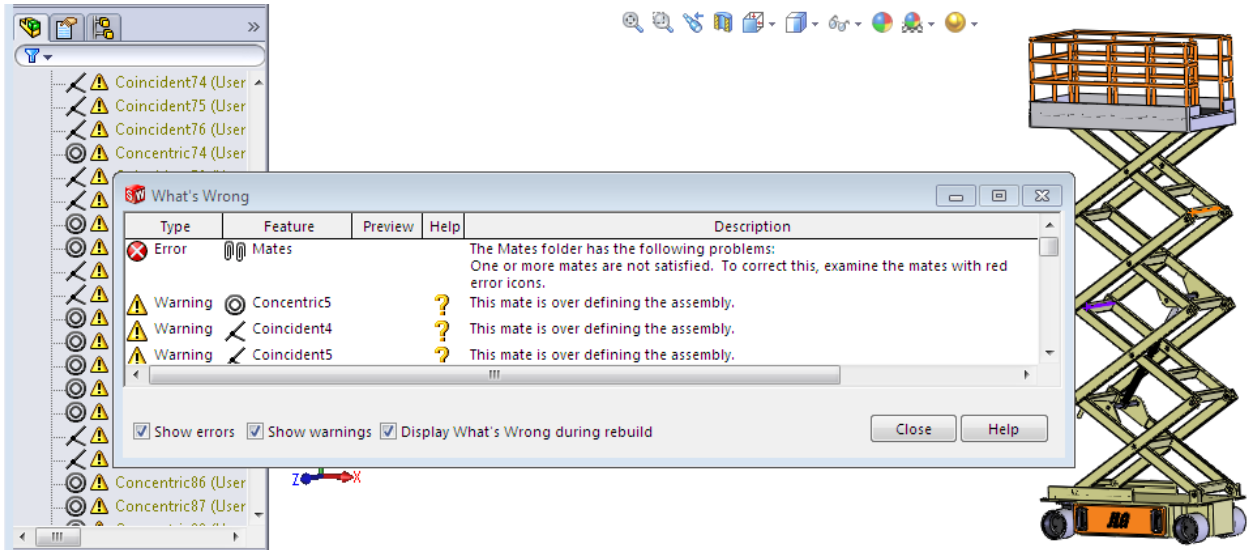


Figure 2: When a new mate is added that results in an inconsistency, previous mates “over defining the assembly” are highlighted. However, the highlighted set is not necessarily minimal. *SolidWorks model from* <http://www.3dcontentcentral.com>.

Potential for algorithmic impact. Given the pebble game algorithms for sparsity in [11], we anticipate our result will lead to efficient approaches for determining the rigidity of body-and-cad frameworks as well as finding rigid components and detecting minimally dependent sets of constraints. *Algorithms based on our characterization would provide the capability of giving valuable feedback to users designing highly complicated CAD systems.*

Related work. Geometric constraint systems are at the core of constraint-based CAD software and have been studied from several perspectives.

In the CAD community, emphasis has been on finding solutions for realizing geometric constraint systems. A common approach is to use a *decomposition-recombination* scheme based on graph algorithms and numerical solvers; see, e.g., [9, 19] for a survey of standard techniques. These decomposition schemes often rely on breaking a system into rigid (also called “well-constrained”) sub-systems. Difficulties arise even in studying small rigid sub-systems. The work of Gao et al. [4] enumerates and analyzes all “basic configurations” with up to six geometric primitives, then presents a method for finding their solutions; the authors observe that the most challenging configurations included constraints involving lines (in contrast to those involving only points or planes).

In classical rigidity theory, bar-and-joint structures composed of universal joints connected by fixed length bars, i.e., point-point distance constraints, are studied. For an overview of combinatorial rigidity theory, see the texts [6, 7].

Combinatorial properties of rigidity are usually tied to *sparsity* counting conditions. A graph G is (k, ℓ) -sparse if the induced subgraph on any subset of n' vertices contains at most $kn' - \ell$ edges. Under certain conditions, there are efficient algorithms to detect (k, ℓ) -sparsity. If G is (k, ℓ) -sparse and $0 \leq \ell < 2k$, then its edges give rise to a matroid. Within this matroidal range of values of k and ℓ , (k, ℓ) -sparsity is determined by a family of pebble game algorithms which run in $O(n^2)$ worst case time [11].

In 2D, bar-and-joint rigidity is characterized by Laman’s theorem with $(2, 3)$ -sparsity; other characterizations followed, some based on decompositions of the edge set into trees [2, 13, 15]. However, 3D bar-and-joint rigidity is not well-understood, and a combinatorial characterization is arguably the biggest open problem in rigidity theory. While $(3, 6)$ -sparsity is necessary, it is not sufficient. Figure 3 depicts the classical “double banana” counterexample; although it satisfies the necessary counts, the structure is flexible, as the “bananas” joined at points a and b can rotate about the dotted axis.

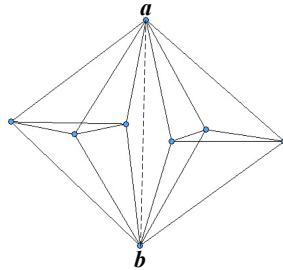


Figure 3: Double banana counterexample shows that $(3, 6)$ -sparsity is not sufficient for 3-dimensional bar-and-joint rigidity. The structure is flexible, as the “bananas” joined at points a and b can rotate about the dotted axis.

While bar-and-joint structures in 3D are not well-understood, a closely related structure called the body-and-bar structure is. The body-and-cad constraints that we consider include point-point distance constraints, which are simply bars – the body-and-bar rigidity model is a special case of body-and-cad. Body-and-bar rigidity was characterized by Tay [20]; an alternate proof was given by White and Whiteley [22]. We generalize White and Whiteley’s proof to obtain our result. Tay’s theorem [20] states that d -dimensional body-and-bar rigidity is equivalent to an associated graph consisting of $\binom{d+1}{2}$ edge-disjoint spanning trees; as a consequence of Nash-Williams and Tutte’s theorems [14, 21] on the equivalence of edge-disjoint spanning trees and sparsity, d -dimensional body-and-bar rigidity is characterized by $((\binom{d+1}{2}), (\binom{d+1}{2}))$ -sparsity.

Other constraints motivated by CAD applications have been studied in rigidity theory. Servatius and Whiteley give a combinatorial characterization of rigidity for frameworks with direction (orientation of

the vector defined by two points with respect to a global coordinate frame) and distance constraints [18]. However, angular constraints among points, even in the plane, have proven very challenging; in [16] Saliola and Whiteley showed that deciding independence of circle intersection angles in the plane has the same complexity as determining 3D bar-and-joint rigidity. Angular constraints between lines and planes or rigid bodies, though, is well-understood [12].

The results from the rigidity theory community have not been directly applied in CAD research partly because rigidity for CAD systems has not yet been fully characterized, and partly because of issues related to *genericity* (discussed in detail in Section 5.1). Note that if a framework is rigid, then the set of all rigid frameworks with the same combinatorics is an open subset of its parameter space. Michelucci and Foufou [1] use this observation and present probabilistic algorithms which rely on analyzing a generic “witness” which shares the incidence constraints of the original system, but may have different parameters for the distance and angular constraints. Even in the plane, where Laman’s theorem characterizes bar-and-joint rigidity, the restriction of genericity poses a subtle challenge. The work of Jermann et al [23] observes that coincidence constraints, when expressed as distance constraints with value 0, exhibit non-generic behavior; a similar situation arises for parallel constraints. This is addressed through a notion of “extended structural rigidity”; Jermann et al make assumptions similar to the genericity conditions for the characterization we present in this paper.

The foundations of *infinitesimal body-and-cad rigidity theory* were introduced in [8]. From the development of a rigidity matrix, a natural *nested sparsity* condition was identified as a necessary, but not sufficient condition for rigidity. The example given there highlighted the need for a better understanding of angular constraints. The need for special treatment of angular constraints was implicitly observed in [5], but, to the best of our knowledge, there has been no other work providing an explicit understanding of their behavior. With both the flavor of 3-dimensional bar-and-joint and body-and-bar rigidity, the question remained as to where the difficulty of body-and-cad rigidity lay. The results we present here provide an answer for the majority of body-and-cad constraints, but indicate that point-point coincidences may pose a significant challenge (see Section 5.2).

Structure. In Section 2, we provide the preliminary concepts necessary for understanding the foundations of infinitesimal body-and-cad rigidity and give an example to highlight the distinct behavior of angular constraints. In Section 3, we develop the rigidity matrix for a more general combinatorial object called a (k, g) -frame, which is used to prove our main theorem in Section 4. In Section 5, we discuss the subtleties and limitations resulting from genericity assumptions as well as the challenges posed by point-point coincidence constraints. We conclude with future work in Section 6.

2 Preliminaries

For a geometric constraint model, there are three levels of rigidity theory: **algebraic**, **infinitesimal** and **combinatorial**. In **algebraic rigidity theory**, a system of equations expressing the geometric constraints is studied; a solution to this system corresponds to a *realization* of the structure¹. In **infinitesimal rigidity theory**, the first-order behavior of the (usually quadratic) system of equations expresses the constraints in terms of instantaneous motions and a *rigidity matrix*. In **combinatorial rigidity theory**, rigidity is defined in terms of the rank of this rigidity matrix, so that *generically* rigidity depends only on properties of a certain graph. *In this paper, we are concerned only with infinitesimal and combinatorial body-and-cad rigidity.*

The **infinitesimal body-and-cad rigidity theory** was first presented in [8] and relies on expressing constraints in the Grassmann-Cayley algebra through the rows of a *rigidity matrix*. For completeness, we provide an overview of the foundations developed in [8].

Body-and-cad constraints. The body-and-cad frameworks that arise from CAD software are naturally 3-dimensional. There are 21 coincidence, angular and distance constraints that can be placed between a pair of geometric elements (points, lines or planes) on rigid bodies, which we enumerate below for clarity:

- **Point-point constraints.** Coincidence, distance.

¹In Appendix C, we provide the formal definitions associated with body-and-cad algebraic rigidity theory, including the family of “length” functions required to describe the geometry of the system.

- **Point-line constraints.** Coincidence, distance.
- **Point-plane constraints.** Coincidence, distance.
- **Line-line constraints.** Parallel, perpendicular, fixed angle, coincidence, distance.
- **Line-plane constraints.** Parallel, perpendicular, fixed angle, coincidence, distance.
- **Plane-plane constraints.** Parallel, perpendicular, fixed angle, coincidence, distance.

Infinitesimal constraint equations. To derive equations from the geometric constraints, we must first consider instantaneous rigid body motion in \mathbb{R}^3 . As a consequence of Chasles’ Theorem (see, e.g., [17]), any instantaneous rigid body motion may be described by a *twist* (translation and rotation about a specified *twist axis*), which itself is represented by a 6-vector $\mathbf{s} = (\boldsymbol{\omega}, \mathbf{v})$. The 3-vector $\boldsymbol{\omega}$ describes the *angular velocity*: the direction of the twist axis and rotational speed about it. The 3-vector \mathbf{v} can be used to decode the rest of the twist axis and translational speed along it.

A *primitive* constraint between two bodies i and j is encoded by a single homogeneous linear equation on the twists $\mathbf{s}_i = (\boldsymbol{\omega}_i, \mathbf{v}_i)$ and $\mathbf{s}_j = (\boldsymbol{\omega}_j, \mathbf{v}_j)$. Each body-and-cad constraint is associated to a number of primitive constraints (which intuitively affect at most one degree of freedom)². A distinction is made between primitive *angular* and *blind* constraints: a primitive angular constraint may affect only a rotational degree of freedom, while a primitive blind constraint may affect either a rotational or translational degree of freedom. Equations corresponding to angular constraints have zeroes in the coordinates corresponding to \mathbf{v} .

The main contribution of [8] was the algebro-geometric derivation of these equations which are collected together in the rigidity matrix to express the infinitesimal body-and-cad constraints. Given a structure with n bodies, the matrix has $6n$ columns; these are arranged so that the 6 columns for the i th vertex correspond to $(\mathbf{v}_i, -\boldsymbol{\omega}_i)$ ³. **For the combinatorial characterization that we present in this paper, we are only concerned with the pattern of non-zero entries in the rigidity matrix.**

Elements of the kernel of the rigidity matrix may be interpreted as the *infinitesimal motions* of the framework. If the only infinitesimal motions are *trivial*, i.e., assign the same twist to each body, the framework is *infinitesimally rigid*; otherwise, it is *infinitesimally flexible*. Since we will only work in the infinitesimal rigidity theory, for brevity, we will drop “infinitesimally” for the remainder of this paper. A *minimally rigid* framework is one that is rigid, but becomes flexible after the removal of any (primitive) constraint.

Example. We provide a small example to illustrate the concepts of **primitive** constraints and their further separation into **angular** and **blind** constraints. To emphasize that we are only concerned with the pattern of zero and non-zero entries, we use *-entries to indicate values that are generically non-zero.

The body-and-cad framework depicted in Figure 1a is composed of two bodies (a cube and hexagonal prism) sharing three constraints: (i) a line-line coincidence, (ii) a point-plane coincidence and (iii) a point-point distance. This example is minimally rigid; for instance, removal of the (primitive blind) point-point distance constraint results in a flexible structure with one degree of freedom (see Figure 1b).

The constraints for this framework are infinitesimally expressed via a rigidity matrix with the pattern depicted in Figure 4. Observe that the line-line coincidence constraint is associated to four rows of the matrix; this corresponds to four **primitive** constraints. In fact, rows 1 and 2 express a line-line parallel constraint and have 0 values in three columns associated with each body; each of these rows is expressing a **primitive angular** constraint. The remaining four rows express **primitive blind** constraints.

Novelty. We emphasize the two main differences between the development of the infinitesimal rigidity theory for the body-and-cad [8] and body-and-bar [20, 22] models. In the rigidity matrix associated to a **body-and-bar** framework, each row corresponds to a bar, or equivalently, a distance constraint between two bodies. By contrast, in order to encode a single constraint in a **body-and-cad** framework, we may need *multiple rows* in the rigidity matrix; the concept of primitive constraints addresses this by associating exactly one constraint with each row.

The second difference appears in the separate treatment of primitive angular and blind constraints, represented by red and black edges, respectively, in a primitive cad graph, defined below. This was the

²Four basic constraints, described in more detail in Appendix A, expressed 20 of the constraints; in Appendix B, we discuss why we cannot address point-point constraints with our proof technique.

³The re-ordering and negation are technicalities arising from the development of the rigidity matrix.

	\mathbf{v}_1	$-\omega_1$	\mathbf{v}_2	$-\omega_2$
line-line coincidence	000	***	000	***
	000	***	000	***
	***	***	***	***
	***	***	***	***
point-plane distance	***	***	***	***
point-point distance	***	***	***	***

Figure 4: The pattern of the rigidity matrix for the structure depicted in Figure 1a.

main challenge left open by the natural *nested sparsity* condition identified as a necessary, but not sufficient, condition for body-and-cad rigidity. The example given on page 27 of [8] highlighted the need for a better understanding of the interplay of angular and blind constraints.

2.1 The primitive cad graph

The infinitesimal theory of [8] lets us associate a *primitive cad graph* $H = (V, B \sqcup R)$ to each body-and-cad framework. Here, H is a multigraph with a vertex for each body and an edge for each primitive constraint. Moreover, the edges are partitioned into two sets, a set B of black edges and a set R of red edges, representing primitive blind and angular constraints, respectively. See Figure 5 for the primitive cad graph associated to the minimally rigid framework in Figure 1.

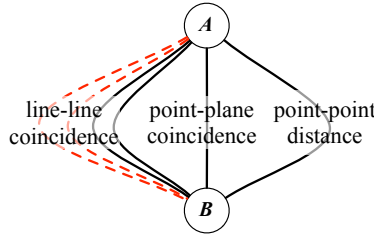


Figure 5: The primitive cad graph associated to the framework from Figure 1a has 2 red (dashed) edges, representing primitive angular constraints, and 4 black (solid) edges, representing primitive blind constraints.

Recall that each primitive constraint is expressed as a single linear equation. In fact, this equation can be encoded by a 6-vector whose entries are derived from the specific geometry of the framework. We define a *primitive cad framework* $H(\mathbf{p})$ to be the graph H in which each edge is labeled with this 6-vector. Let m be the number of edges in H and $m_R = |R|$ be the number of red edges. Our main theorem for 3-dimensional body-and-cad rigidity is stated in terms of the primitive cad graph H .

Theorem 1. *A 3-dimensional body-and-cad framework (in which no point-point coincidence constraints are present) is generically minimally rigid if and only if, in its associated primitive cad graph $H = (V, R \sqcup B)$, there is some set of black edges $B' \subseteq B$ such that*

1. $B \setminus B'$ is the edge-disjoint union of 3 spanning trees, and
2. $R \cup B'$ is the edge-disjoint union of 3 spanning trees.

Body-and-cad frameworks are a special case of the more general (k, g) -frames introduced in Section 3. Theorem 1 follows from a result (Theorem 16) in this more general setting, which we prove in Section 4.

3 From body-and-cad frameworks to (k, g) -frames

We begin in Section 3.1 by introducing the (k, g) -frame, which generalizes both the notion of a body-and-cad framework and the k -frame of [22], and its associated rigidity matrix. We then present a pure condition

for the minimal rigidity of a (k, g) -frame in Section 3.2. From the point of view of applications, our result is most interesting for 3-dimensional body-and-cad frameworks; however, the techniques do not depend on dimension, so we work in the most general setting.

3.1 (k, g) -frames

The proof of our main result depends only on the pattern of zeroes in the rigidity matrix of a body-and-cad framework, and not on their derivation or interpretation. Thus, we may view the pattern in the rigidity matrix associated to a primitive cad framework as an instance of a rigidity matrix associated to a more general (k, g) -frame, which we introduce below. We begin with some preliminary combinatorial definitions.

Definition 2. A multigraph $H = (V, E = B \sqcup R)$ is a bi-colored graph, where $V = \{1, \dots, n\}$ is the vertex set, and E is a set of m edges, m_B of which are black and m_R of which are red. For brevity, we use “graphs” to refer to multigraphs.

We generalize the notion of a k -frame in Definition 1.7 of [22].

Definition 3. A (k, g) -frame $H(\mathbf{p})$ is a bi-colored graph $H = (V, E = B \sqcup R)$ together with a function $\mathbf{p} : E \rightarrow \mathbb{R}^k$, where $\mathbf{p}(r)_j = 0$ for $j = 1, \dots, k - g$ and $r \in R$.

Then, primitive cad frames in 3D are simply $(6, 3)$ -frames. The k -frames of White and Whiteley are (k, g) -frames in which R is empty (hence the value of g is irrelevant).

Associated to each (k, g) -frame is a rigidity matrix which we define below.

Definition 4. Given a (k, g) -frame $H(\mathbf{p})$, we define a matrix $M(H(\mathbf{p}))$ with k columns per vertex. For each edge $e = uv$ with $u < v$, define a row with $\mathbf{p}(e)$ in the k columns for u and $-\mathbf{p}(e)$ in the k columns for v .

Motions assign a vector of length k to each body; for structures in dimension d , $k = \binom{d+1}{d}$, and each vector represents a compatible infinitesimal motion.

Definition 5. A motion of a (k, g) -frame is a vector of length kn that is orthogonal to the row space of $M(H(\mathbf{p}))$. A trivial motion assigns the same k -vector to each body, i.e., has n copies of the same k -vector.

We are concerned with *minimal rigidity*, i.e., structures with no redundant constraints.

Definition 6. A (k, g) -frame $H(\mathbf{p})$ is minimally rigid⁴ if it becomes flexible after the removal of any edge from H .

Remark 7. Definitions 3 and 4 set the pattern of zeroes in the matrix $M(H(\mathbf{p}))$. However, the rows of the body-and-cad rigidity matrix presented in [8] are more specialized. In Appendix A we give an alternative derivation of equations for two of the basic body-and-cad constraints so that the equations conform to the pattern we have set.

3.2 The pure condition for minimal rigidity

As with other classical rigidity results, our characterization relies solely on the *combinatorics* of a body-and-cad framework, which applies *generically*. In this section we introduce the pure condition for the minimal rigidity of a (k, g) -frame, generalizing the setup in [22]. In fact, the existence of a pure condition is what justifies our genericity assumptions, which we discuss in more detail in Section 5.1.

The definition below generalizes necessary edge-counting conditions for minimal rigidity, taking angular constraints into account.

Definition 8. Let k and g be positive integers. A bi-colored graph H is (k, g) -counted if

1. $m = kn - k$ (count on total edges), and
2. $m_R \leq gn - g$ (count on red edges).

⁴Also called “isostatic” in the literature.

The matrix $M(H(\mathbf{p}))$ of a (k, g) -counted (k, g) -frame is not square (it has $kn - k$ rows and kn columns). It is straightforward to observe that any minimally rigid (k, g) -frame must have $kn - k$ rows since the trivial motions will always be in the kernel of $M(H(\mathbf{p}))$. If we fix or “tie down” one of the bodies in the framework, then these trivial motions are no longer allowed.

Definition 9. *The basic tie-down of a (k, g) -counted (k, g) -frame is a $k \times kn$ matrix $T(k)$ with the identity matrix in the first k columns and 0s everywhere else.*

Given a (k, g) -counted (k, g) -frame $H(\mathbf{p})$, the (square) matrix $M_T(H(\mathbf{p}))$ is $M(H(\mathbf{p}))$ with $T(k)$ appended to the bottom.

Thus, the rigidity of a (k, g) -frame $H(\mathbf{p})$ satisfying the necessary counts may be determined by computing the determinant of the matrix $M_T(H(\mathbf{p}))$.

Proposition 10 (Proposition 2.5 from [22]). *A (k, g) -counted (k, g) -frame $H(\mathbf{p})$ is minimally rigid if and only if $M_T(H(\mathbf{p})) \neq 0$.*

In fact, since we would like to understand rigidity more generally than for a single set of values for \mathbf{p} , we would like to think of $M_T(H(\mathbf{x}))$ as a polynomial in indeterminates. As in [22], we make the following definition.

Definition 11. *Given a (k, g) -frame $H(\mathbf{p})$, we define the generic (k, g) -frame $H(\mathbf{x})$ on the underlying labeled graph H by setting all generically non-zero entries of the k -vectors labeling the edges to be algebraically independent indeterminates $\mathbf{x}(b)_j$ for $j = 1, \dots, k$, and $\mathbf{x}(r)_j$ for $j = k - g + 1, \dots, k$, where $b \in B$ and $r \in R$.*

We define the *pure condition* to be $C_H(\mathbf{x}) = \det M_T(H(\mathbf{x}))$ so that $C_H(\mathbf{x})$ is a polynomial in $N = km_B + gm_R$ variables. Generic rigidity is expressed in terms of the pure condition.

Definition 12. *A (k, g) -counted (k, g) -frame $H(\mathbf{x})$ is generically minimally rigid if there exists a function $\mathbf{p} : E \rightarrow \mathbb{R}^k$ for which $C_H(\mathbf{p}) \neq 0$ satisfying $\mathbf{p}(r)_i = 0$ for $i = 1, \dots, k - g$ for all $r \in R$.*

We require one final combinatorial concept for analyzing the pure condition.

Definition 13. *A (k, g) -fan ϕ of a (k, g) -counted bicolored graph is a partitioning of E into $n - 1$ ordered sets (ϕ_2, \dots, ϕ_n) such that*

1. *each $\phi_i = (\phi_{i,1}, \dots, \phi_{i,k})$ contains exactly k edges incident to vertex i , and*
2. *each ϕ_i contains $\leq g$ (red) edges from R .*

We denote the determinant of the matrix whose rows are $\mathbf{x}(\phi_{i,1}), \dots, \mathbf{x}(\phi_{i,k})$ by $[\phi_i]$.

Definition 14. *Two (k, g) -fans ϕ and ϕ' are called distinct if there exists a vertex i such that $\phi_i \neq \phi'_i$, as unordered sets.*

We can represent distinct (k, g) -fans by orienting H : if edge $e \in \phi_i$, orient it so that its tail is at vertex i . Then, given a (k, g) -fan (ϕ_2, \dots, ϕ_n) , its (k, g) -fan diagram is the oriented multigraph $F = (V, A)$, where $\vec{ij} \in A$ if and only if $ij \in \phi_i$. Note that the same (k, g) -fan diagram will represent multiple (k, g) -fans, as depicted in Figure 6b, but exactly one distinct (k, g) -fan.

As a consequence of Proposition 2.12 from [22], we obtain the following.

Proposition 15. $C_H(\mathbf{x}) = \Sigma_{\phi} \pm [\phi_2] \cdots [\phi_n]$, for all distinct (k, g) -counted (k, g) -fans ϕ of H .

Proof. If we compute $\det M_T(H(\mathbf{x}))$ via a Laplace expansion on the first k columns of $M_T(H(\mathbf{x}))$, we see that the determinant is actually the determinant of the $(kn - k) \times (kn - k)$ matrix formed by deleting the first k columns and last k rows. We can in turn compute the determinant of this submatrix via a Laplace expansion taking the k columns of each vertex at a time. This requires that we compute the determinant of matrices formed by partitioning the rows of our matrix so that k rows are associated to each vertex $2, \dots, n$. Each row corresponds to an edge, and if we have a submatrix containing more than g rows associated to red edges, then the corresponding determinant is zero. Therefore, $C_H(\mathbf{x})$ is the sum of terms of the form $\pm [\phi_2] \cdots [\phi_n]$, where $\phi = (\phi_2, \dots, \phi_n)$ is a distinct (k, g) -fan. The sign of each term is determined by the rules for Laplace expansion, the permutation ϕ , and whether the vectors used in the Laplace expansion are $\mathbf{x}(e)$ or $-\mathbf{x}(e)$. \square

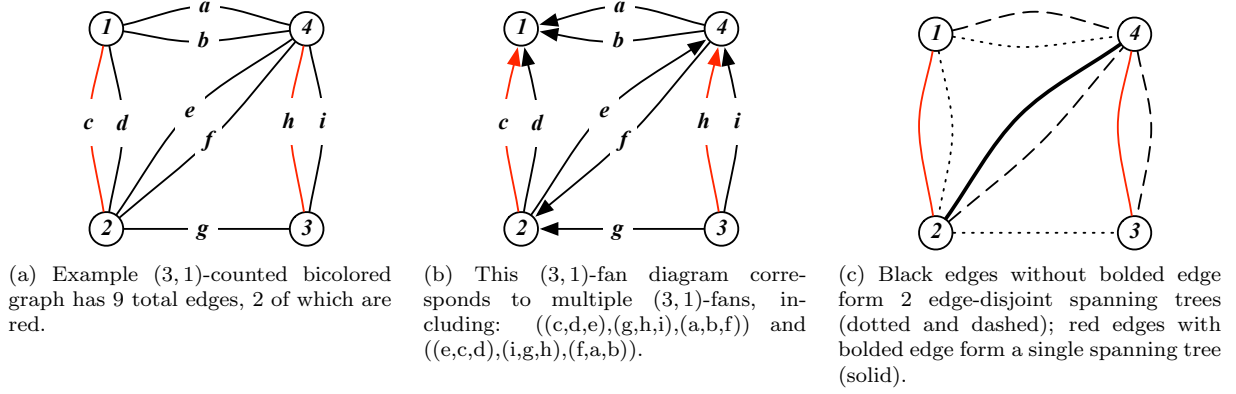


Figure 6: An example $(3,1)$ -counted graph satisfying the conditions of Theorem 16. The graph has two red edges: c between vertices 1 and 2, and h between vertices 3 and 4.

4 A combinatorial characterization of minimal rigidity

Given the setup of [8] and the previous sections, our main result may be stated and proved in a purely combinatorial setting. Theorem 16 and its proof are a generalization of the body-and-bar characterization theorem of White and Whiteley.

Theorem 16. *A (k,g) -counted (k,g) -frame $H(\mathbf{x})$ is generically minimally rigid if and only if there exists some set of black edges $B' \subseteq B$ such that*

1. $B \setminus B'$ is the edge-disjoint union of $k - g$ spanning trees, and
2. $R \cup B'$ is the edge-disjoint union of g spanning trees.

Figure 6c depicts an example of a $(3,1)$ -counted bi-colored graph satisfying the conditions of Theorem 16.

Proof. (\implies) Assume $C_H(\mathbf{x}) \neq 0$. Consider a Laplace expansion along the last k rows of $M_T(H(\mathbf{x}))$. Since the only non-zero entries in these rows occur in the $k \times k$ identity matrix appearing in the tie-down in the first k columns, $\det M_T(H(\mathbf{x})) = \det A$, where A is the submatrix of $M_T(H(\mathbf{x}))$ formed by the first $kn - k$ rows and last $kn - k$ columns. Since $C_H(\mathbf{x}) = \det M_T(H(\mathbf{x}))$, then $\det A \neq 0$.

Now consider a Laplace expansion of $\det A$ using $(n-1) \times (n-1)$ -minors so that $\det A$ is a sum of terms $\mu = \det A_1 \cdots \det A_k$, where for $j = 1, \dots, k$, A_j is an $(n-1) \times (n-1)$ submatrix of A using the j th columns associated to each of the $n-1$ remaining vertices and some choice of $n-1$ rows. If $\det A$ is non-zero, then some term $\mu = \det A_1 \cdots \det A_k$ is non-zero, which implies that $\det A_1, \dots, \det A_k$ are all non-zero. Each submatrix A_j has one column per vertex, and the rows of A_j are just the rows of the incidence matrix of an orientation on the edges of H multiplied by non-zero scalars. Since $\det A_j$ is non-zero, A_j is the incidence matrix of a subgraph of H with $n-1$ edges and no cycles. Hence, A_j describes a spanning tree T_j of H .

If r is a red edge, then $\mathbf{x}(r)_j = 0$ for $j = 1, \dots, k-g$. Since $\det A_j$ is non-zero for all j , the edge r must be in one of the trees T_{k-g+1}, \dots, T_k . Let $B' \subseteq B$ be the set of black edges in T_{k-g+1}, \dots, T_k . Then $B \setminus B'$ is the edge-disjoint union of T_1, \dots, T_{k-g} and $R \cup B'$ is the edge-disjoint union of the g remaining spanning trees.

(\impliedby) Let $H(\mathbf{x})$ be the generic (k,g) -frame, where $H = (V, E = B \sqcup R)$ is a (k,g) -counted graph, and let $B' \subseteq B$ be a set of edges such that

1. $B \setminus B'$ is the edge-disjoint union of $k - g$ spanning trees T_1, \dots, T_{k-g} ,
2. $R \cup B'$ is the edge-disjoint union of g spanning trees T_{k-g+1}, \dots, T_k .

We show that $\det M_T(H(\mathbf{x}))$ is not identically zero. To do this it suffices to show that there exists a function $\mathbf{x}' : E \rightarrow \mathbb{R}^k$ such that $\det M_T(H(\mathbf{x}')) \neq 0$. For $j = 1, \dots, k$ and $i = 1, \dots, k$, let $a_{j,i}$ denote an indeterminate. For each j and $e \in T_j$ let

$$\mathbf{x}'(e) = \begin{cases} (a_{j,1}, a_{j,2}, \dots, a_{j,k}) & \text{if } e \in B \setminus B' \\ (0, 0, \dots, 0, a_{j,k-g+1}, \dots, a_{j,k}) & \text{if } e \in R \cup B' \end{cases}$$

By Proposition 15, $C_H(\mathbf{x}) = \Sigma_\phi \pm \Pi_{i=2}^n [\phi_i]$. We claim that the only non-zero term in the pure condition stems from a single distinct (k, g) -fan ϕ . Root each tree at vertex 1. Each tree has a unique path from vertex i to the root, so we can orient all edges toward the root. Define ϕ_i to be the ordered set of all edges incident to vertex i pointing toward the root, where the j th edge in ϕ_i is the edge in T_j . By construction, each ϕ_i has at most g red edges, so $[\phi_i] \neq 0$.

Consider another distinct (k, g) -fan $\phi' \neq \phi$. There must be some vertex i such that ϕ'_i contains at least two edges e_1 and e_2 from the same tree T_j . Hence, $\mathbf{x}'(e_1) = \mathbf{x}'(e_2)$ and $[\phi'_i] = 0$, and we conclude that ϕ is the only fan for which $\Pi_{i=2}^n [\phi_i]$ is non-zero. \square

We now prove Theorem 1, which gives a combinatorial characterization for 3-dimensional body-and-cad rigidity (omitting point-point coincidence constraints).

Proof of Theorem 1. The result follows from Theorem 16 as a primitive cad graph for a body-and-cad framework with no point-point coincidence constraints is a (k, g) -frame with $k = 6$ and $g = 3$. \square

5 Considerations and challenges

Before concluding, we discuss practical implications of the genericity assumptions that result from the pure condition, then provide context as to why point-point coincidence constraints pose a challenge.

5.1 Genericity

Like all combinatorial characterizations of rigidity, our main theorem gives a condition for *generic* minimal rigidity. This notion of genericity is subtle as there are currently no geometric conditions implying or characterizing it (even in the most well-studied bar-and-joint rigidity model). Common assumptions in computational geometry, such as the general position of joint coordinates, are not strong enough to ensure the genericity of a bar-and-joint structure, and we have additional types of constraints to consider. Thus it is difficult to test when a given framework satisfies the genericity assumptions needed for the combinatorial analysis.

We defined generic rigidity using the pure condition (see Definition 12) and now discuss why this definition is appropriate. Recall that $N = km_B + gm_R$. The set of all points $\mathbf{q} \in \mathbb{R}^N$ with $C_H(\mathbf{q}) = 0$ is a closed subset that either has dimension less than N or is all of \mathbb{R}^N . Consequently, the set of points $\mathbf{q} \in \mathbb{R}^N$ such that $C_H(\mathbf{q}) \neq 0$ is open. This implies that, if there exists one $\mathbf{q} \in \mathbb{R}^N$ such that $C_H(\mathbf{q}) \neq 0$, then the pure condition is non-zero for all points in some small neighborhood of \mathbf{q} . Moreover, if $C_H(\mathbf{q}) \neq 0$ for some \mathbf{q} , then the set of points with $C_H(\mathbf{q}) = 0$ is a *proper* closed subset of \mathbb{R}^N with measure zero, and $C_H(\mathbf{q}') \neq 0$ *generically*, i.e., for almost all values $\mathbf{q}' \in \mathbb{R}^N$.

Therefore, Definition 12 can be viewed as an extension of Tay's notion of generic rigidity [20] to (k, g) -frames. A (k, g) -frame $H(\mathbf{x})$ is generically minimally rigid if and only if $C_H(\mathbf{x})$ is not identically zero. If, however, $C_H(\mathbf{x})$ is not the zero polynomial and $C_H(\mathbf{p}) = 0$ for some $\mathbf{p} \in \mathbb{R}^N$, then $H(\mathbf{p})$ is (infinitesimally) flexible. We refer to \mathbf{p} as a *non-generic* point, and say that we have a non-generic embedding of the (k, g) -frame $H(\mathbf{p})$. If the polynomial $C_H(\mathbf{x})$ is identically zero, then $H(\mathbf{x})$ is *generically flexible*.

A non-generic framework: Pappus's Theorem

As observed by Jermann et al [23], there are inherent problems in analyzing the geometry of a specific realization of a framework using only the combinatorics of a graph, as a particular embedding or framework may fail to be generic.

This problem is straightforward to observe in the analysis of body-and-bar frameworks, in which all constraints are point-point distance constraints. For example, consider a graph with vertices v_1 and v_2

joined by 6 edges; this is the combinatorial model for two rigid bodies joined by 6 bars. If the bars are attached at points that are chosen generically, then the framework is rigid, matching the combinatorial analysis provided by Tay’s Theorem [20]. However, if the points are not sufficiently generic – for example if

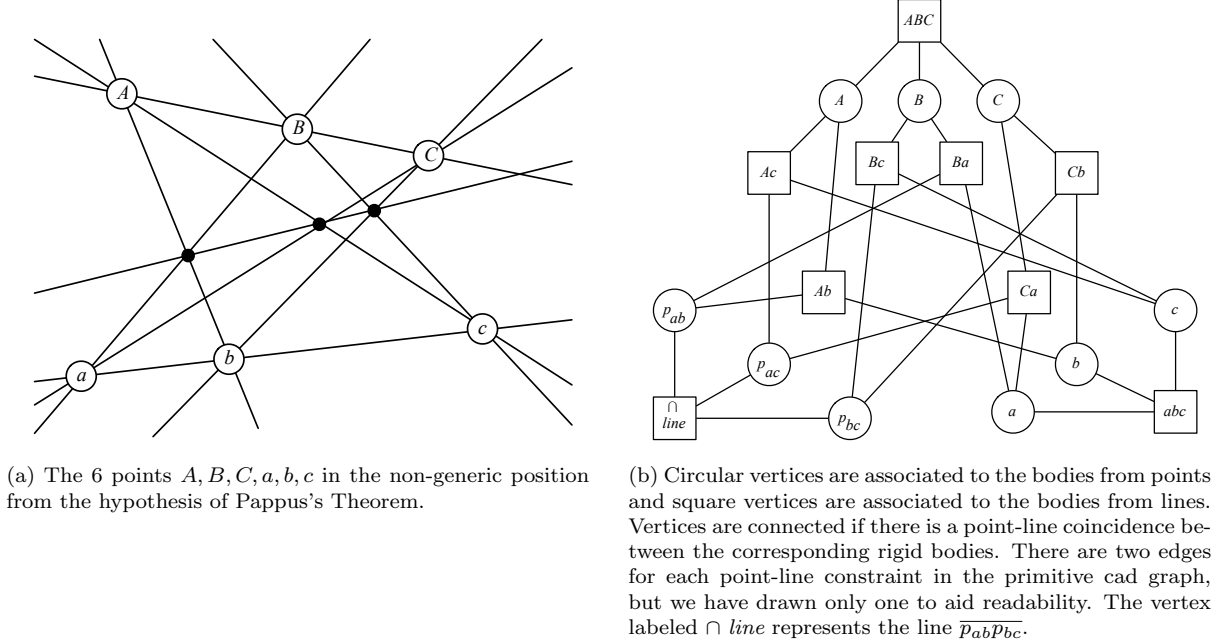


Figure 7: The point-line coincidences described by Pappus’s Theorem.

all 6 bars attach to a single point on one of the bodies – then the framework is flexible; for this *non-generic* embedding, Tay’s theorem does not apply. Intuitively, “reusing” the same point results in a dependency that is not encountered in the generic case.

The constraints in a body-and-cad framework present similar challenges in applying combinatorial analysis. To illustrate this, we present a body-and-cad framework along with a non-generic embedding, modeling Pappus’ Theorem, in which a generically independent constraint becomes dependent.

Theorem 17 (Pappus). (See Figure 7a.) Let A, B, C and a, b, c be two sets of 3 collinear points in the plane. Then the 3 points $p_{ab} = Ab \cap Ba$, $p_{ac} = Ac \cap Ca$, and $p_{bc} = Bc \cap Cb$ are collinear.

To model Pappus’s Theorem, we use a framework with 18 bodies: 9 to model the points, and another 9 to model the two lines \overline{ABC} and \overline{abc} , the six lines $\overline{Ab}, \overline{Ac}, \overline{Ba}, \overline{Bc}, \overline{Ca}, \overline{Cb}$, and the line $\overline{p_{ab}p_{bc}}$. If we encode all of the point-line coincidences depicted in diagram (a) in Figure 7, then the point-line coincidence between p_{ac} and $\overline{p_{ab}p_{bc}}$ is implied by the other constraints as a consequence of Pappus’s Theorem. Thus, there is a *dependency* among the geometric constraints which should correspond to a dependency in the rigidity matrix.

However, a combinatorial analysis of the associated primitive cad graph (depicted schematically in Figure 7b) based on Theorem 1 indicates that the constraints are *generically* independent. Indeed, we can create a generic embedding of the same primitive cad graph in which each constraint uses unique geometric elements: for each point-line coincidence, identify a distinct point and distinct line on the pair of constrained bodies. If the 27 points and 27 lines are sufficiently generic, then the associated rigidity matrix has full rank, and the constraints are generically independent.

5.2 Point-point coincidence constraints

The result given in this paper does not address point-point coincidence constraints. In addition to the algebraic difficulties (described in Appendix B) that prohibit the inclusion of point-point coincidence constraints

in the definition of a (k, g) -frame, point-point coincidences seem inherently more challenging to address.

It may be that characterizing 3D point-point coincidences is just as challenging as understanding 3D bar-and-joint rigidity. Indeed, we can construct an analogue of the classical “double banana” example with a body-and-cad framework that has two rigid bodies joined by two point-point coincidence constraints. The two rigid bodies are free to rotate about the line joining their two points of intersection (labeled \vec{a} and \vec{b} in Figure 3), so the body-and-cad framework is flexible.

In this example, each point-point coincidence constraint corresponds to three primitive blind constraints (see Appendix B), and the primitive cad graph contains 2 vertices and 6 black edges between them. A natural extension of Theorem 1 would characterize generic minimal rigidity with a partitioning of the edge set into 6 edge-disjoint spanning trees (there are no red edges). While this property is necessary, it is not sufficient. The primitive cad graph for the “double banana” satisfies the condition, but is flexible, thus serving as a counterexample. Therefore, a combinatorial characterization of *body-and-cad* frameworks including point-point coincidences must differ from the characterization for body-and-cad frameworks presented here.

6 Conclusions and Future Work

We have presented a combinatorial characterization of body-and-cad rigidity of structures using 20 of the 21 pairwise constraints; we exclude point-point coincidence constraints. This characterization is expressed in terms of the edge set of an associated graph being partitioned into two sets of 3 edge-disjoint spanning trees.

Future work and open problems. The discussion in Section 5.1 highlights a practical, but notoriously difficult, problem in rigidity theory: determine geometric necessary or sufficient conditions for a specific embedding of a body-and-cad framework to be generic.

We suspect that analyzing point-point coincidences in body-and-cad frameworks may be just as hard as analyzing 3D bar-and-joint rigidity. Understanding precisely where the challenge lies merits a comprehensive investigation, and the relationship between 2D body-and-cad and 2D bar-and-joint structures is a natural starting point.

Algorithms. The combinatorial property of Theorem 16 must be matroidal as it characterizes the independence of rows in a matrix. Due to the intimate relation between edge-disjoint spanning trees and sparsity counts, we expect to obtain efficient algorithms for body-and-cad rigidity by generalizing the pebble game algorithms. Such algorithms would not only **decide** whether a given framework is rigid or flexible, but should be able to **detect rigid components and circuits**, minimally dependent sets of (primitive) constraints. This would provide valuable feedback to CAD users when the addition of a constraint causes an inconsistency.

References

- [1] Dominique Michelucci and Sebt Foufou, *Detecting all dependences in systems of geometric constraints using the witness method* (Francisco Botana and Tomás Recio, eds.), Lecture Notes in Computer Science, vol. 4869, Springer, 2007.
- [2] Henry Crapo, *On the generic rigidity of plane frameworks*, Technical Report 1278, Institut de recherche d’informatique et d’automatique, 1988.
- [3] Dassault Systèmes, *Solidworks: 3d mechanical design and 3d CAD software*, 2010. <http://www.solidworks.com/>.
- [4] Xiao-Shan Gao, Christoph M. Hoffmann, and Wei-Qiang Yang, *Solving spatial basic geometric constraint configurations with locus intersection*, Proceedings of the seventh acm symposium on solid modeling and applications, 2002, pp. 95–104.
- [5] Xiao-Shan Gao, Qiang Lin, and Gui-Fang Zhang, *A c-tree decomposition algorithm for 2d and 3d geometric constraint solving*, Computer-Aided Design **38** (2006), no. 1, 1–13.
- [6] Jack Graver, Brigitte Servatius, and Herman Servatius, *Combinatorial rigidity* (James E. Humphreys, Robion C. Kirby, and Lance Small, eds.), Graduate Studies in Mathematics, vol. 2, American Mathematical Society, 1993.
- [7] Jack E. Graver, *Counting on frameworks: Mathematics to aid the design of rigid structures*, Mathematical Association of America, 2001.
- [8] Kirk Haller, Audrey Lee-St.John, Meera Sitharam, Ileana Streinu, and Neil White, *Body-and-cad geometric constraint systems*, Computational Geometry: Theory and Applications **45** (2012), no. 8, 385–405.

- [9] Christophe Jermann, Gilles Trombettoni, Bertrand Neveu, and Pascal Mathis, *Decomposition of geometric constraint systems: a survey*, Int. J. Comput. Geometry Appl. **16** (2006), no. 5-6, 379–414.
- [10] Gerard Laman, *On graphs and rigidity of plane skeletal structures*, Journal of Engineering Mathematics **4** (1970), 331–340.
- [11] Audrey Lee and Ileana Streinu, *Pebble game algorithms and sparse graphs*, Discrete Mathematics **308** (2008), no. 8, 1425–1437.
- [12] Audrey Lee-St.John and Ileana Streinu, *Angular rigidity in 3d: combinatorial characterizations and algorithms*, Proceedings of the 21st canadian conference on computational geometry (cccg2009), 2009, pp. 67–70.
- [13] László Lovász and Y. Yemini, *On generic rigidity in the plane*, SIAM J. Algebraic and Discrete Methods **3** (1982), no. 1, 91–98.
- [14] C. St. J. A. Nash-Williams, *Edge-disjoint spanning trees of finite graphs.*, Journal London Math. Soc. **36** (1961), 445–450.
- [15] András Recski, *A network theory approach to the rigidity of skeletal structures ii. laman’s theorem and topological formulae.*, Discrete Applied Math **8** (1984), 63–68.
- [16] Franco Saliola and Walter Whiteley, *Constraining plane configurations in cad: Circles, lines, and angles in the plane*, SIAM J. Discrete Math. **18** (2004), no. 2, 246–271.
- [17] J. M. Selig, *Geometric fundamentals of robotics*, 2nd ed., Monographs in Computer Science series, Springer, New York, 2005.
- [18] Brigitte Servatius and Walter Whiteley, *Constraining plane configurations in computer-aided design: Combinatorics of directions and lengths*, SIAM J. Discrete Math. **12** (1999), no. 1, 136–153.
- [19] Meera Sitharam, *Combinatorial approaches to geometric constraint solving: Problems, progress, and directions*, Geometric and algorithmic aspects of computer-aided design and manufacturing, 2005, pp. 117–163.
- [20] Tiong-Seng Tay, *Rigidity of multi-graphs. I. Linking rigid bodies in n -space*, Combinatorial Theory Series **B** (1984), no. 26, 95–112.
- [21] William T. Tutte, *On the problem of decomposing a graph into n connected factors*, Journal London Math. Soc. **142** (1961), 221–230.
- [22] Neil White and Walter Whiteley, *The algebraic geometry of motions of bar- and-body frameworks*, SIAM Journal of Algebraic Discrete Methods **8** (1987), 1–32.
- [23] C. Jermann, B. Neveu, and G. Trombettoni, *A new structural rigidity for geometric constraint systems* (F. Winkler, ed.), Lecture Notes in Computer Science, vol. 2930, Springer, 2004.

A Alternative development of body-and-cad rigidity matrix

In [8], a body-and-cad rigidity matrix was developed by expressing each of 20 possible 3-dimensional constraints in terms of four basic constraints:

- (i) *basic line-line non-parallel fixed angular*,
- (ii) *basic line-line parallel*,
- (iii) *basic blind orthogonality*, and
- (iv) *basic blind parallel*.

Point-point coincidence constraints required a separate development, and the resulting rows do not have the pattern of generically non-zero entries required for the (k, g) -frames in this paper.

Constraints (i) and (ii) are *angular* constraints, as the corresponding twists have $\mathbf{v} = 0$. Each basic constraint corresponds to either one or two rows in the rigidity matrix.

The **basic angular** constraint (i) requires that the angle between two vectors \mathbf{a} and \mathbf{b} be maintained. This constraint corresponds to a single row in the rigidity matrix of the form

$$\begin{array}{ccccccc} \cdots & \mathbf{v}_i & -\boldsymbol{\omega}_i & \cdots & \mathbf{v}_j & -\boldsymbol{\omega}_j & \cdots \\ \cdots 0 \cdots & \mathbf{0} & \mathbf{b} \times \mathbf{a} & \cdots 0 \cdots & \mathbf{0} & \mathbf{a} \times \mathbf{b} & \cdots 0 \cdots \end{array}$$

Constraint (ii) requires a line to be parallel to a line in a fixed direction $\mathbf{c} = (c_1, c_2, c_3)$. This condition translates into two rows:

$$\begin{array}{ccccccc} \cdots & \mathbf{v}_i & -\boldsymbol{\omega}_i & \cdots & \mathbf{v}_j & -\boldsymbol{\omega}_j & \cdots \\ \cdots 0 \cdots & \mathbf{0} & (-c_2, c_1, 0) & \cdots 0 \cdots & \mathbf{0} & (c_2, -c_1, 0) & \cdots 0 \cdots \\ \cdots 0 \cdots & \mathbf{0} & (0, -c_3, c_2) & \cdots 0 \cdots & \mathbf{0} & (0, c_3, -c_2) & \cdots 0 \cdots \end{array}$$

The reverse direction of the proof of Theorem 16 requires us to assume that, except for the vectors \mathbf{v} that are required to be zero in angular constraints, all other entries of the rigidity matrix are generically non-zero. Therefore, this representation of constraint (ii) is incompatible with the proof.

However, since (ii) is expressing a line-line parallel constraint, we have an alternate description. Let \mathbf{a} and \mathbf{b} be two directions such that $\mathbf{a} \times \mathbf{b} = \mathbf{c}$. Then constraint (ii) can be expressed using two rows, each of which reduce to basic constraint (i):

$$\begin{array}{ccccccc} \cdots & \mathbf{v}_i & -\boldsymbol{\omega}_i & \cdots & \mathbf{v}_j & -\boldsymbol{\omega}_j & \cdots \\ \cdots 0 \cdots & \mathbf{0} & \mathbf{c} \times \mathbf{a} & \cdots 0 \cdots & \mathbf{0} & \mathbf{a} \times \mathbf{c} & \cdots 0 \cdots \\ \cdots 0 \cdots & \mathbf{0} & \mathbf{c} \times \mathbf{b} & \cdots 0 \cdots & \mathbf{0} & \mathbf{b} \times \mathbf{c} & \cdots 0 \cdots \end{array}$$

For the **basic blind** constraints, let \mathbf{p} be a point, \mathbf{p}' its instantaneous velocity resulting from a twist and $\mathbf{c} = (c_1, c_2, c_3)$ a direction vector. Then (iii) expressed that \mathbf{p}' must be orthogonal to \mathbf{c} , and was associated to a single row

$$\begin{array}{ccccccc} \cdots & \mathbf{v}_i & -\boldsymbol{\omega}_i & \cdots & \mathbf{v}_j & -\boldsymbol{\omega}_j & \cdots \\ \cdots 0 \cdots & (\mathbf{p} : 1) \vee (\mathbf{c} : 0) & & \cdots 0 \cdots & -(\mathbf{p} : 1) \vee (\mathbf{c} : 0) & & \cdots 0 \cdots \end{array}$$

Constraint (iv) expressed that \mathbf{p}' must be parallel to \mathbf{c} and was associated to two rows

$$\begin{array}{ccccccc} \cdots & \mathbf{v}_i & -\boldsymbol{\omega}_i & \cdots & \mathbf{v}_j & -\boldsymbol{\omega}_j & \cdots \\ \cdots 0 \cdots & (\mathbf{p} : 1) \vee (c_2, -c_1, 0, 0) & & \cdots 0 \cdots & -(\mathbf{p} : 1) \vee (c_2, -c_1, 0, 0) & & \cdots 0 \cdots \\ \cdots 0 \cdots & (\mathbf{p} : 1) \vee (0, c_3, -c_2, 0) & & \cdots 0 \cdots & -(\mathbf{p} : 1) \vee (0, c_3, -c_2, 0) & & \cdots 0 \cdots \end{array}$$

As in constraint (ii), in constraint (iv) we are requiring that two vectors, \mathbf{p}' and \mathbf{c} be parallel. Again, there is an alternate description. Indeed, let \mathbf{a} and \mathbf{b} be two directions such that $\mathbf{a} \times \mathbf{b} = \mathbf{c}$. Then constraint (iv) can be expressed using two rows, each of which reduces to basic constraint (iii):

$$\begin{array}{ccccccc} \cdots & \mathbf{v}_i & -\boldsymbol{\omega}_i & \cdots & \mathbf{v}_j & -\boldsymbol{\omega}_j & \cdots \\ \cdots 0 \cdots & (\mathbf{p} : 1) \vee (\mathbf{a} : 0) & & \cdots 0 \cdots & -(\mathbf{p} : 1) \vee (\mathbf{a} : 0) & & \cdots 0 \cdots \\ \cdots 0 \cdots & (\mathbf{p} : 1) \vee (\mathbf{b} : 0) & & \cdots 0 \cdots & -(\mathbf{p} : 1) \vee (\mathbf{b} : 0) & & \cdots 0 \cdots \end{array}$$

We conclude that, generically, the entries in the three ω columns for **basic angular** constraints (i) and (ii) are non-zero, and the entries in the six \mathbf{v} and ω columns for **basic blind** constraints (iii) and (iv) are non-zero. Therefore, the body-and-cad rigidity matrix resulting from this alternative development will satisfy the definition of a (6, 3)-frame (as per Definition 3).

B Point-point coincidence constraints

In this section, we provide some insight as to why we are unable to treat point-point coincidence constraints. If $\mathbf{p} = (p^x, p^y, p^z)$ is the point of coincidence, then the constraint is infinitesimally expressed by 3 rows in the rigidity matrix of the form:

$\dots \mathbf{0} \dots$	$(1, 0, 0, 0, -p^z, p^y)$	$\dots \mathbf{0} \dots$	$(-1, 0, 0, 0, p^z, -p^y)$	$\dots \mathbf{0} \dots$
$\dots \mathbf{0} \dots$	$(0, 1, 0, p^z, 0, -p^x)$	$\dots \mathbf{0} \dots$	$(0, -1, 0, -p^z, 0, p^x)$	$\dots \mathbf{0} \dots$
$\dots \mathbf{0} \dots$	$(0, 0, 1, -p^y, p^x, 0)$	$\dots \mathbf{0} \dots$	$(0, 0, -1, p^y, -p^x, 0)$	$\dots \mathbf{0} \dots$

Since these rows do not conform to the pattern required by our proof technique, point-point coincidences are not addressed by the characterization.

C Body-and-cad algebraic rigidity theory

For completeness, we include the definitions from [8] required to express the geometry of a body-and-cad structure, from which the algebraic theory is derived. A *cad graph* (G, c) is used to represent the combinatorics of the constraints, where $G = (V, E)$ is a multigraph with $V = \{1, \dots, n\}$ and $c : E \rightarrow C$ is an edge coloring using colors $C = \{c_1, \dots, c_{21}\}$ to denote the 21 possible cad constraints. This is related to the *primitive cad graph* presented in Section 2.1: for each color c_i , we associate some number of primitive angular and primitive blind constraints as found in Table 1 (reproduced from [8]). The bi-colored primitive cad graph $H = (V, E = B \sqcup R)$ has a red edge for each primitive angular constraint and a black edge for each primitive blind constraint.

	point		line		plane	
	angular	blind	angular	blind	angular	blind
point						
coincidence	0	3	0	2	0	1
distance	0	1	0	1	0	1
line						
coincidence			2	2	1	1
distance			0	1	1	1
parallel			2	0	1	0
perpendicular			1	0	2	0
fixed angular			1	0	1	0
plane						
coincidence					2	1
distance					2	1
parallel					2	0
perpendicular					1	0
fixed angular					1	0

Table 1: Association of body-and-cad (*coincidence*, *angular*, *distance*) constraints with the number of blind and angular primitive constraints. As an example of how to read the table, the last two columns (corresponding to **plane**) of row 3 (corresponding to **coincidence** under **line**) indicate that a **line-plane coincidence** constraint reduces to 1 angular and 1 blind primitive constraint.

The geometry of the constraint represented by each cad graph edge is given in terms of points, lines, or planes affixed to the n rigid bodies; each line or plane may be described by a point on a rigid body and a direction vector. Let E_i denote the set of edges of color c_i . Then we define a “length” function L_i that associates to each edge in E_i the real-valued points, vectors and values (e.g., specified distance or angle) needed to describe the constraint; the full description of the family of functions L_i is below. With these definitions, we can formally define a *body-and-cad framework* to be $(G, c, L) = (G, c, L_1, \dots, L_{21})$, the cad graph (G, c) together with the functions L_i .

- **Point-point coincidence:** $L_1 : E_1 \rightarrow \mathbb{R}^3$ maps an edge $e = ij$ to a point \vec{p} so that it is constrained to lie on bodies i and j simultaneously.
- **Point-point distance:** $L_2 : E_2 \rightarrow \mathbb{R}^3 \times \mathbb{R}^3 \times \mathbb{R}$ maps an edge $e = ij$ to a triple $(\vec{p}_i, \vec{p}_j, a)$ so that the point \vec{p}_i affixed to body i is constrained to lie a distance a from the point \vec{p}_j affixed to body j .
- **Point-line coincidence:** $L_3 : E_3 \rightarrow \mathbb{R}^3 \times (\mathbb{R}^3 \times \mathbb{R}^3)$ maps an edge $e = ij$ to a pair $(\vec{p}_i, (\vec{p}_j, \vec{d}))$ so that point \vec{p}_i affixed to body i is constrained to lie on the line (\vec{p}_j, \vec{d}) affixed to body j .
- **Point-line distance:** $L_4 : E_4 \rightarrow \mathbb{R}^3 \times (\mathbb{R}^3 \times \mathbb{R}^3) \times \mathbb{R}$ maps an edge $e = ij$ to a triple $(\vec{p}_i, (\vec{p}_j, \vec{d}), a)$ so that point \vec{p}_i affixed to body i is constrained to lie a distance a from the line (\vec{p}_j, \vec{d}) affixed to body j .
- **Point-plane coincidence:** $L_5 : E_5 \rightarrow \mathbb{R}^3 \times (\mathbb{R}^3 \times \mathbb{R}^3)$ maps an edge $e = ij$ to a pair $(\vec{p}_i, (\vec{p}_j, \vec{d}))$ so that the point \vec{p}_i affixed to body i is constrained to lie in the plane (\vec{p}_j, \vec{d}) affixed to body j .
- **Point-plane distance:** $L_6 : E_6 \rightarrow \mathbb{R}^3 \times (\mathbb{R}^3 \times \mathbb{R}^3) \times \mathbb{R}$ maps an edge $e = ij$ to a triple $(\vec{p}_i, (\vec{p}_j, \vec{d}), a)$ so that the point \vec{p}_i affixed to body i is constrained to lie a distance a from the plane (\vec{p}_j, \vec{d}) affixed to body j .
- **Line-line parallel:** $L_7 : E_7 \rightarrow \mathbb{R}^3 \times \mathbb{R}^3 \times \mathbb{R}^3$ maps an edge $e = ij$ to a triple $(\vec{p}_i, \vec{p}_j, \vec{d})$ so that the lines (\vec{p}_i, \vec{d}) and (\vec{p}_j, \vec{d}) affixed to bodies i and j , respectively, are constrained to remain parallel to each other.
- **Line-line perpendicular:** $L_8 : E_8 \rightarrow (\mathbb{R}^3 \times \mathbb{R}^3) \times (\mathbb{R}^3 \times \mathbb{R}^3)$ maps an edge $e = ij$ to a pair $((\vec{p}_i, \vec{d}_i), (\vec{p}_j, \vec{d}_j))$ so that the lines (\vec{p}_i, \vec{d}_i) and (\vec{p}_j, \vec{d}_j) affixed to bodies i and j , respectively, are constrained to remain perpendicular to each other.
- **Line-line fixed angular:** $L_9 : E_9 \rightarrow (\mathbb{R}^3 \times \mathbb{R}^3) \times (\mathbb{R}^3 \times \mathbb{R}^3) \times \mathbb{R}$ maps an edge $e = ij$ to a triple $((\vec{p}_i, \vec{d}_i), (\vec{p}_j, \vec{d}_j), \alpha)$ so that the lines (\vec{p}_i, \vec{d}_i) and (\vec{p}_j, \vec{d}_j) affixed to bodies i and j , respectively, are constrained to maintain the angle α between them.
- **Line-line coincidence:** $L_{10} : E_{10} \rightarrow \mathbb{R}^3 \times \mathbb{R}^3$ maps an edge $e = ij$ to a pair (\vec{p}, \vec{d}) so that the line (\vec{p}, \vec{d}) is constrained to be affixed to bodies i and j simultaneously.
- **Line-line distance:** $L_{11} : E_{11} \rightarrow (\mathbb{R}^3 \times \mathbb{R}^3) \times (\mathbb{R}^3 \times \mathbb{R}^3) \times \mathbb{R}$ maps an edge $e = ij$ to a triple $((\vec{p}_i, \vec{d}_i), (\vec{p}_j, \vec{d}_j), a)$ so that the lines (\vec{p}_i, \vec{d}_i) and (\vec{p}_j, \vec{d}_j) affixed to bodies i and j , respectively, are constrained to lie a distance a from each other.
- **Line-plane parallel:** $L_{12} : E_{12} \rightarrow (\mathbb{R}^3 \times \mathbb{R}^3) \times (\mathbb{R}^3 \times \mathbb{R}^3)$ maps an edge $e = ij$ to a pair $((\vec{p}_i, \vec{d}_i), (\vec{p}_j, \vec{d}_j))$ so that the line (\vec{p}_i, \vec{d}_i) and plane (\vec{p}_j, \vec{d}_j) affixed to bodies i and j , respectively, are constrained to remain parallel to each other.
- **Line-plane perpendicular:** $L_{13} : E_{13} \rightarrow (\mathbb{R}^3 \times \mathbb{R}^3) \times (\mathbb{R}^3 \times \mathbb{R}^3)$ maps an edge $e = ij$ to a pair $((\vec{p}_i, \vec{d}_i), (\vec{p}_j, \vec{d}_j))$ so that the line (\vec{p}_i, \vec{d}_i) and plane (\vec{p}_j, \vec{d}_j) affixed to bodies i and j , respectively, are constrained to remain perpendicular to each other.
- **Line-plane fixed angular:** $L_{14} : E_{14} \rightarrow (\mathbb{R}^3 \times \mathbb{R}^3) \times (\mathbb{R}^3 \times \mathbb{R}^3) \times \mathbb{R}$ maps an edge $e = ij$ to a triple $((\vec{p}_i, \vec{d}_i), (\vec{p}_j, \vec{d}_j), \alpha)$ so that the line (\vec{p}_i, \vec{d}_i) and plane (\vec{p}_j, \vec{d}_j) affixed to bodies i and j , respectively, are constrained to maintain the angle α between them.

- **Line-plane coincidence:** $L_{15} : E_{15} \rightarrow (\mathbb{R}^3 \times \mathbb{R}^3) \times (\mathbb{R}^3 \times \mathbb{R}^3)$ maps an edge $e = ij$ to a pair $((\vec{p}_i, \vec{d}_i), (\vec{p}_j, \vec{d}_j))$ so that the line (\vec{p}_i, \vec{d}_i) affixed to body i is constrained to lie in the plane (\vec{p}_j, \vec{d}_j) affixed to body j .
- **Line-plane distance:** $L_{16} : E_{16} \rightarrow (\mathbb{R}^3 \times \mathbb{R}^3) \times (\mathbb{R}^3 \times \mathbb{R}^3) \times \mathbb{R}$ maps an edge $e = ij$ to a triple $((\vec{p}_i, \vec{d}_i), (\vec{p}_j, \vec{d}_j), a)$ so that the line (\vec{p}_i, \vec{d}_i) affixed to body i is constrained to lie a distance a from the plane (\vec{p}_j, \vec{d}_j) affixed to body j .
- **Plane-plane parallel:** $L_{17} : E_{17} \rightarrow \mathbb{R}^3 \times \mathbb{R}^3 \times \mathbb{R}^3$ maps an edge $e = ij$ to a triple $(\vec{p}_i, \vec{p}_j, \vec{d})$ so that the planes (\vec{p}_i, \vec{d}) and (\vec{p}_j, \vec{d}) affixed to bodies i and j , respectively, are constrained to remain parallel to each other.
- **Plane-plane perpendicular:** $L_{18} : E_{18} \rightarrow (\mathbb{R}^3 \times \mathbb{R}^3) \times (\mathbb{R}^3 \times \mathbb{R}^3)$ maps an edge $e = ij$ to a pair $((\vec{p}_i, \vec{d}_i), (\vec{p}_j, \vec{d}_j))$ so that the planes (\vec{p}_i, \vec{d}_i) and (\vec{p}_j, \vec{d}_j) affixed to bodies i and j , respectively, are constrained to remain perpendicular to each other.
- **Plane-plane fixed angular:** $L_{19} : E_{19} \rightarrow (\mathbb{R}^3 \times \mathbb{R}^3) \times (\mathbb{R}^3 \times \mathbb{R}^3) \times \mathbb{R}$ maps an edge $e = ij$ to a triple $((\vec{p}_i, \vec{d}_i), (\vec{p}_j, \vec{d}_j), \alpha)$ so that the planes (\vec{p}_i, \vec{d}_i) and (\vec{p}_j, \vec{d}_j) affixed to bodies i and j , respectively, are constrained to maintain the angle α between them.
- **Plane-plane coincidence:** $L_{20} : E_{20} \rightarrow \mathbb{R}^3 \times \mathbb{R}^3$ maps an edge $e = ij$ to the pair (\vec{p}, \vec{d}) so that the plane (\vec{p}, \vec{d}) is constrained to be affixed to both bodies i and j simultaneously.
- **Plane-plane distance:** $L_{21} : E_{21} \rightarrow \mathbb{R}^3 \times \mathbb{R}^3 \times \mathbb{R}^3 \times \mathbb{R}$ maps an edge $e = ij$ to a quadruple $(\vec{p}_i, \vec{p}_j, \vec{d}, a)$ so that the planes (\vec{p}_i, \vec{d}) and (\vec{p}_j, \vec{d}) affixed to bodies i and j , respectively, are constrained to have the distance a between them.